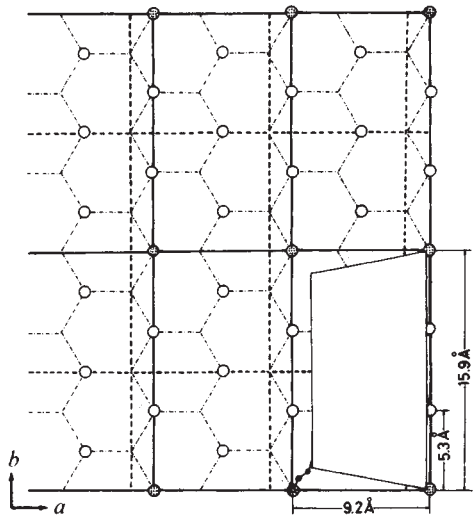

Fig. 3 An idealized relationship between the arrangements of the POH groups and CDen molecules in the inter-layer space of α-zirconium phosphate (projection on the a-b plane). The upward-pointing POH groups in the lower layer are represented by circles and the downward-pointing ones in the upper layer are located at the triple points of dash-dot lines. Each CDen molecule with its cavity axis parallel to the a axis anchors through the basic terminus to the POH site (shaded for the lower layer) and is placed in the rectangle surrounded by the solid (lower layer) or broken (upper layer) lines.

diameter and 8.0 Å in the thickness of the torus, are intercalated as a bi-layer with their cavity axes perpendicular or parallel to the phosphate layers. Assuming hexagonal close packing of CDen molecules in a plane perpendicular to their cavity axes, the effective area per molecule is evaluated as $2\sqrt{3}\times(15.4/2)^2$ or 205 Å^2. The effective area per POH site in α-ZrP is 24.3 Å^2 (ref. 7). Hence, the maximum values of x and Δ for the perpendicular arrangement can be calculated, respectively, as $2\times 24.3/205 = 0.24$ and as twice 11.8 Å, which is the sum of the thickness of the torus and the extended chain length of the aminoethylamino group, or 23.6 Å. These calculations are not consistent with the observed data. On the other hand, the parallel arrangement yields a maximum x value of $2\times 24.3/(15.8\times 8.0) = 0.40$ and a minimum Δ value of $15.4(1+\sqrt{3/2}) = 28.7$ Å, in fairly close agreement with the observations. Thus, we propose the model shown in Fig. 2 as the probable arrangement of CDen molecules in the inter-layer space of α-ZrP. This model gives a ξ value for sample A of $0.368/0.40 = 92.0\%$, which is close to the value roughly estimated from the X-ray observations. It can also be assumed that sample A is a mixture of 92 mol% of a complex, $Zr(HPO_4)_2(CDen)_{0.4}\cdot 5.7H_2O$, and 8 mol% of α-ZrP.

Referring to the crystal structure of α-ZrP, the POH groups pointing up or down in each layer are located in a monoclinic cell with dimensions of 9.2 and 5.3 Å along the a and b axes, respectively[6], as shown in Fig. 3. Any two adjacent layers of ZrP are staggered in such a way that the downward-pointing POH groups in the upper layer are shifted by 3.07 Å along the a axis relative to the layer below. It is therefore conceivable that the first intercalated layer of CDen molecules, with their cavity axes parallel to the a axis of the α-ZrP crystal, anchors through the basic termini to every POH site, at 9.2-Å intervals, in every sixth row, 15.9 Å apart, along this axis in the ZrP layer below. The second intercalated layer is probably bonded in the same manner to the ZrP layer above, but is shifted by 7.7 and 8.0 Å along the a and b axes, respectively, relative to the first layer. Thus, the parallel bi-layer model suggested above is also consistent with the geometrical arrangement of POH sites at the inorganic layer surface.

Depending on the size and ionic or molecular character of the substrate, the cyclodextrins and their adducts are crystallized as empty molecules or as inclusion complexes, with channel or cage structures in which the cyclodextrin molecules are stacked like coins in a roll or arranged in a herring-bone pattern[5]. The channel structure is formed only as inclusion complexes with long-chain molecules such as poly-iodine. As the hydrate of β-cyclodextrin contains 7 water molecules within the cavity[9], it is probable that $0.4\times 7/5.3 = 49\%$ of the water molecules in sample A are located in the cavity of the intercalated CDen molecules. According to thermo-gravimetric observations, this sample released 85 mol% of its water during heating to 120 °C, and the dehydrated solid re-adsorbed 92 mol% of the desorbed water by exposure to saturated water vapour at 25 °C, followed by air-drying under the same conditions as for sample A. These preliminary results and the above geometrical considerations suggest that the CDen molecules in one intercalated layer are arranged with their cavity axes parallel to the inter-layer surface, either in alignment to form empty channels, 6 Å in diameter, or, if displaced, with bottlenecks large enough to allow water molecules 2.65 Å in diameter to diffuse. Thus, the dextrin moiety of the CDen-ZrP may possess a zeolitic character, at least for small molecules such as water and hydrogen, although definite conclusions must await further work. Complexes of α-zirconium phosphate with CDen or other cyclodextrin derivatives may prove useful as solid supports in gas or liquid chromatography and as micro-encapsulating agents for various substances such as drugs.

Received 31 December 1985; accepted 15 May 1986.

1. Pinnavaia, T. J. *Science* **220**, 365-371 (1983).
2. Ferragina, C., Massucci, M. A., Patrono, P., Ginestra, A. L. & Tomlinson, A. A. G. *JCS Dalton Trans.*, 265-271 (1986).
3. Kijima, T., Tanaka, J., Goto, M. & Matsui, Y. *Nature* **310**, 45-47 (1984).
4. Kijima, T., Kobayashi, M. & Matsui, Y. *J. Inclusion Phenom.* **2**, 807-813 (1985).
5. Saenger, W. *Angew. Chem.* **19**, 344-362 (1980).
6. Alberti, G. & Constantino, U. in *Intercalation Chemistry* (eds Whittingham, M. S. & Jacobson, A. J.) Ch. 5 (Academic, New York, 1982).
7. Kijima, T. *Thermochim. Acta* **59**, 95-104 (1982).
8. Kijima, T., Ueno, S. & Goto, M. *JCS Dalton Trans.*, 2499-2503 (1982).
9. Linder, K. & Saenger, W. *Angew. Chem.* **17**, 694-695 (1978).

Plume versus lithospheric sources for melts at Ua Pou, Marquesas Islands

R. A. Duncan*‡, M. T. McCulloch*, H. G. Barsczus† & D. R. Nelson*

* Research School of Earth Sciences, The Australian National University, Canberra, ACT 2601, Australia
† ORSTOM, Centre de Papeete Tahiti, French Polynesia, and Géologique et Géophysique du CCNRS, USTL, Montpellier, France
§ Permanent address: College of Oceanography, Oregon State University, Corvallis, Oregon 97331, USA

The remarkable distinction between the compositions of ocean island basalts (OIBs) and mid-ocean ridge basalts (MORBs) provides an important constraint on models of mantle composition and structure[1-3]. Previous studies of OIBs[4-8], however, have emphasized regional isotopic variations, often relying on a small number of samples from many separate volcanoes. Although this type of sampling has now established the basic range of isotopic variations, with the notable exception of the Hawaiian Islands[6,9,10], there is little information on either spatial or temporal variations within a single volcano. Here we report isotopic (Sr, Nd and Pb) and K–Ar age measurements for tholeiites, alkali basalts and differentiated rocks from the island of Ua Pou. In this island volcanism spanned the interval from 5.6 to 1.8 Myr, with the ratio of highly to moderately incompatible trace elements increasing

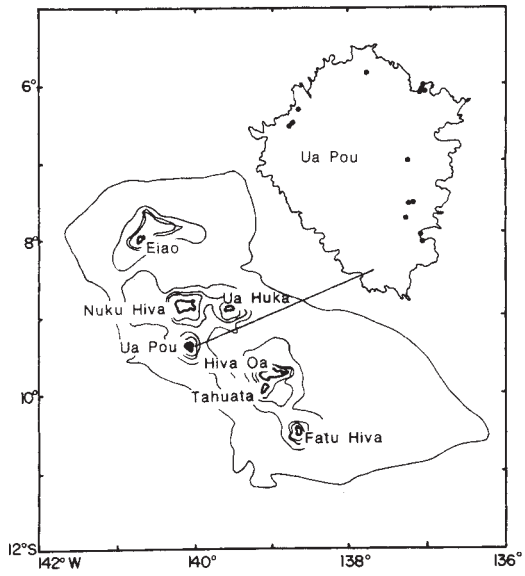

Fig. 1 Map of the Marquesas Islands, an age-progressive volcanic lineament in the south-central Pacific basin, showing the island of Ua Pou. Solid circles (on the enlarged map of the island) mark the location of samples (tholeiites, alkali basalts and differentiates) analysed in the present study.

with time; however, in contrast to Hawaii, $^{87}Sr/^{86}Sr$ and $^{207}Pb/^{204}Pb$ increased while $^{143}Nd/^{144}Nd$ decreased from the tholeiitic to alkalic magmas. The total variation in isotopic composition within this single island is nearly as great as within the entire French Polynesian region[8,11,12], and argues against systematic geographical correlations[13].

The island of Ua Pou, at 9°24′ S, 140°04′ W, is one of a chain of more than 20 volcanic islands and seamounts which constitute the Marquesas archipelago in the south-central Pacific Basin (Fig. 1). These volcanoes are linearly arrayed in a WNW–ESE direction, sub-parallel with other young intra-plate Pacific island chains. This characteristic geometry and the reported southeasterly progression in volcano ages[14,15], from 6.3 to 1.4 Myr, has linked Marquesan volcanism to a hotspot origin. The abyssal (>4,000 m) ocean floor on which these islands were constructed formed at the Galapagos Rise (ancestral East Pacific Rise) between 50 and 60 Myr (ref. 16).

Ua Pou hosts a particularly wide range of rock compositions, from tholeiitic to alkalic basalts; the latter have undergone low-pressure fractionation towards trachytic and phonolitic rocks[17,18]. Although tholeiites are the main rock type in the Hawaiian islands[19], they have not been reported elsewhere in the French Polynesian region; their occurrence in the initial stage of volcanism at Ua Pou suggests that tholeiitic eruptions may occur throughout this region, but may be almost totally confined to submarine portions of the volcanoes.

We report here age determinations for rocks from Ua Pou. Previous age studies[14] on other islands from the Marquesas chain have documented an age progression in volcanism from north-west to south-east at a rate of ~10.4 cm yr^{-1} (ref. 9). From this regular age distribution along the lineament, the expected age range at Ua Pou is 4.0–2.7 Myr. Re-examination[20] of the published age data showed that at the islands of Nuku Hiva and Hiva Oa dated rocks defined two age groups separated by about the same timespan, 0.6 Myr. Furthermore, at each island the older group was predominantly olivine tholeiite while the younger group was alkali basalt. To investigate this apparent petrogenetic evolution at individual Marquesan volcanoes, additional sampling was undertaken by one of us (H.G.B.).

Ua Pou does not exhibit the central collapsed caldera commonly seen at other Marquesas Islands; instead, the island's

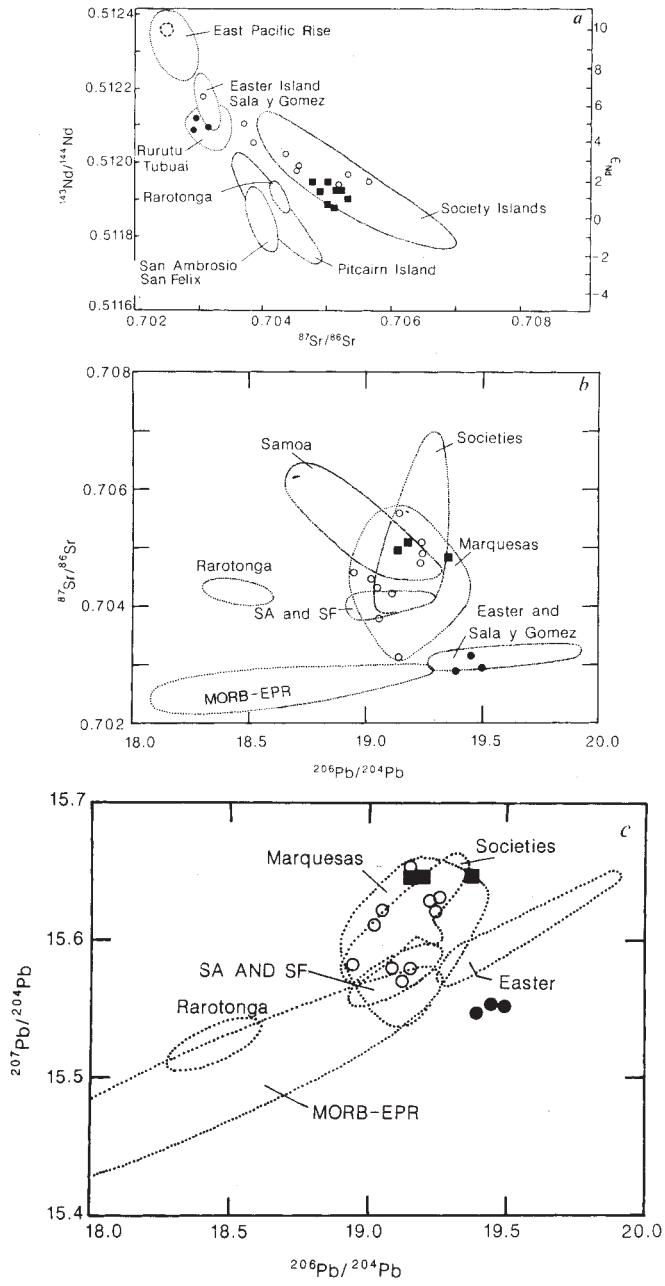

Fig. 2 Isotopic compositions of lavas from Ua Pou compared with those for other basaltic rocks from the south-central Pacific basin. *a*, $^{143}Nd/^{144}Nd$ versus $^{87}Sr/^{86}Sr$; *b*, $^{87}Sr/^{86}Sr$ verus $^{206}Pb/^{204}Pb$; *c*, $^{207}Pb/^{204}Pb$ versus $^{206}Pb/^{204}Pb$. Fields of data are from ref. 25 for islands and East Pacific Rise, except Rurutu and Pitcairn Islands[30]. Solid circles and squares are tholeiites and alkali basalts, respectively, from Ua Pou. Open circles are other analysed samples from the Marquesas Islands[12]. SA, San Ambrosio; SF, San Felix; EPR, East Pacific Rise.

centre is a complex zone of high-level intrusions of trachytic and phonolitic rocks which have obscured the early shield structure of the volcano. Shield lavas outcrop around the perimeter of the island, in stream valleys, in road cuts and along wave-cut cliffs. The samples analysed in this study are well distributed, coming from the northwestern, northern and eastern sides of the island (Fig. 1).

Initial studies[18] of trace element compositions of tholeiites and alkali basalts collected from Ua Pou revealed striking differences in the inferred source compositions for the two groups. Rocks which plot as tholeiites in a standard alkalis versus silica diagram predate the alkali basalt assemblage. The

Table 1 Sr, Nd and Pb isotopic compositions and K-Ar ages for volcanic rocks from Ua Pou, Marquesas Islands

Samples	Rock type	K (%)	Rb (p.p.m.)	Sr (p.p.m.)	Sm (p.p.m.)	Nd (p.p.m.)	$^{87}Sr/^{86}Sr$	$^{143}Nd/^{144}Nd$	ε_{Nd}	$^{206}Pb/^{204}Pb$	$^{207}Pb/^{204}Pb$	$^{208}Pb/^{204}Pb$	K-Ar age (Myr) $\pm 1\sigma$
UAP-011	Tholeiite	0.554	15	548	10.3	43.3	0.70289±2	0.512070±12	+4.6	19.50	15.54	39.15	4.46±0.07
UAP-017	Tholeiite	0.204	3	434	10.0	40.3	0.70294±4	0.512118±16	+5.5	19.39	15.54	38.99	4.51±0.14
UAP-024	Tholeiite	0.651	11	610	13.0	57.6	0.70318±5	0.512084±24	+4.8	19.45	15.55	39.01	5.61±0.06
UAP-001	Alkali basalt	0.871	41	985	11.4	71.4	0.70500±5	0.511944±27	+2.1				2.75±0.03
UAP-002	Alkali basalt	0.554	76	904	11.8	62.4	0.70497±5						2.78±0.03
UAP-003	Alkali basalt	0.855	40	972	11.3	61.5	0.70482±5						2.70±0.06
UAP-010	Alkali basalt	1.039	145	1,235	13.3	76.0	0.70509±5	0.511867±14	+0.6	19.18	15.65	39.31	2.70±0.04
UAP-026	Alkali basalt	0.524	84	910	11.5	60.7	0.70497±5	0.511876±20	+0.8	19.14	15.64	39.20	2.88±0.08
UAP-012	Tephrite	2.640	116	1,373	15.3	84.6	0.70515±5	0.511918±10	+1.6				2.24±0.05
UAP-015	Hawaiite	2.643	241	1,358	7.9	48.6	0.70481±5	0.511907±12	+1.4	19.36	15.65	39.35	1.78±0.03
UAP-025	Mugearite	4.276	72	1,282	13.0	52.2	0.70531±6	0.511891±25	+1.1				2.49±0.03
UAP-004	Trachyte						0.70508±5						
UAP-019	Phonolite	5.693	240	146	15.3	108.0	0.70497±4	0.511917±22	+1.6				2.42±0.04
UAP-037	Phonolite	5.887	235	136	6.9	52.8	0.70474±5						2.42±0.03

$^{87}Sr/^{86}Sr$ and $^{143}Nd/^{144}Nd$ ratios are normalized to $^{86}Sr/^{88}Sr = 0.1194$ and $^{146}Nd/^{142}Nd = 0.636151$, K-Ar ages were calculated using the following decay and abundance constants: $\lambda_e = 0.581 \times 10^{-10}\ yr^{-1}$; $\lambda_\beta = 4.963 \times 10^{-10}\ yr^{-1}$; $^{40}K/K = 1.167 \times 10^{-4}$ mol mol^{-1} respectively. For the standard NBS 987, $^{87}Sr/^{86}Sr = 0.71023$ and for BCR-1 $^{143}Nd/^{144}Nd = 0.511833$. Rb, Sr, Sm and Nd concentrations are from ref. 18.

tholeiitic phase of volcanism (5.6–4.5 Myr) is separated from the alkali basalt eruptions (2.9–2.7 Myr) and subsequent flows and intrusions of liquids evolved by high-level fractional crystallization (2.5–1.8 Myr). The entire age range of subaerial volcanism at Ua Pou is ~3.8 Myr (Table 1). The apparent 1.6-Myr hiatus between the tholeiitic and alkalic stages of volcanism could be the result of incomplete sampling and may be reduced by future geochronological studies on well-mapped sections. The progression from tholeiitic to alkalic volcanism at Ua Pou and its likelihood at the neighbouring islands of Nuku Hiva and Hiva Oa[20] is reminiscent of the volcanic evolution of the Hawaiian Islands[19]. In the Marquesas Islands, however, no very undersaturated, post-erosional eruptions have followed the alkali basalt stage. It is probable, therefore, that each of the Marquesas islands evolved through a common sequence. Initially, eruptions may have been a mixture of tholeiitic and alkalic compositions, as seen at Macdonald[21] seamount at the southeastern end of the Austral Islands, and Loihi seamount[22] in the Hawaiian Islands. Tholeiitic compositions dominated the early shield-building phase, which at Ua Pou barely reached sea level. This was followed by eruptions of alkali basalt and, later, highly evolved rocks. It is not yet known whether the change from tholeiites to alkali basalts occurred as a gradual transition or as a sharp compositional break after a significant hiatus in volcanic activity.

Major and trace element concentrations for Ua Pou rocks have been reported elsewhere[17,18]. Liotard *et al.*[18] identified tholeiitic rocks at many of the Marquesas Islands and, in particular, quartz-normative tholeiites at Ua Pou, in addition to the earlier described alkali basalts. The tholeiites and alkali basalts cannot be related to one another by either variable partial melting from a common source or fractional crystallization from a parental melt, because of many clear differences in their trace element patterns. Both groups are enriched in light rare earth elements, relative to MORBs, but whereas the alkali basalts exhibit uniformly steep patterns, the tholeiitic samples show much flatter profiles between La and Sm. The tholeiite trace element patterns are similar in shape to those for Hawaiian tholeiites[23,24], with normalized La ≈ normalized Ce, but abundances are higher in Ua Pou tholeiites. Tholeiites and alkali basalts at Ua Pou can also be distinguished by Zr/Nb (11.3 versus 4.8, average values, respectively), La/Nb (0.85 versus 0.98) and La/Ce (0.37 versus 0.51). In addition, on a spidergram diagram the tholeiites show significant depletions of Ba, Rb, Th, K and Sr relative to La.

To characterize further the two magma types present at Ua Pou, we have measured Sr, Nd and Pb isotopic compositions (Table 1). Previous isotopic studies of Marquesas Islands rocks[11,12,25] have not recognized the importance of the tholeiites, nor have they examined the compositional variation with age at a single island. Our results are in excellent agreement with the isotopic analyses of alkali basalts from Ua Pou reported by Vidal *et al.*[12]. The data were obtained using separation techniques and mass spectrometric analysis, as described in refs 26 (Sr and Nd) and 27 (Pb). Measured Sr, Nd and Pb isotopic ratios are generally within the analytical uncertainty of initial ratios because of the young age of the samples. Corrections to $^{87}Sr/^{86}Sr$ were applied only to the high Rb/Sr phonolite samples. Our results are plotted on three diagrams: $^{143}Nd/^{144}Nd$ against $^{87}Sr/^{86}Sr$ (Fig. 2*a*), $^{87}Sr/^{86}Sr$ against $^{206}Pb/^{204}Pb$ (Fig. 2*b*), and $^{207}Pb/^{204}Pb$ against $^{206}Pb/^{204}Pb$ (Fig. 2*c*).

Tholeiites are distinguishable from alkali basalts and differentiated rocks using each of the three isotopic systems. The strontium composition of the tholeiites is among the least radiogenic reported from oceanic islands, while the alkali basalt $^{87}Sr/^{86}Sr$ values fall in the middle of the range for other Marquesas and Society Islands[8,11,12]. The corresponding $^{143}Nd/^{144}Nd$ values are also distinctive ($\varepsilon_{Nd} = 4.6$–5.5 for tholeiites verus 0.6–2.1 for alkali basalts) and, together with the Sr data, form an array parallel to the Society Islands compositions but oblique to the mantle array[5–8]. The extreme isotopic heterogeneity of the French Polynesian region has been noted, but at Ua Pou, as recognized for Nuku Hiva by Vidal *et al.*[12], nearly the entire range of variability exists on the scale of a single island. At Ua Pou the tholeiitic magmas have low $^{87}Sr/^{86}Sr$ ratios and moderate $^{143}Nd/^{144}Nd$ ratios, indicative of a mantle source with low time-integrated Rb/Sr and a (chondrite-normalized) Nd/Sm < 1. The later alkali basalt magmas have high $^{87}Sr/^{86}Sr$ and low $^{143}Nd/^{144}Nd$, which would derive from a less depleted mantle source. This contrasts with the Hawaiian Islands volcanism, where the tholeiites have higher $^{87}Sr/^{86}Sr$ and lower ε_{Nd} values than the alkali basalts and post-erosional lavas[9,10].

The Pb compositions of the two magma types are equally distinct, as seen in the $^{207}Pb/^{204}Pb$ versus $^{206}Pb/^{204}Pb$ diagram (Fig. 2*c*). The tholeiites are most similar to rocks from Easter and Sala y Gomez Islands near the East Pacific Rise[25], whereas the alkali basalts lie in the field of other reported Pb isotopic analyses from the Society and Marquesas Islands[12,25]. The Pb isotopic compositions of the Ua Pou tholeiites are not as extreme as those of rocks from Tubuai[12] (Austral Islands) which exhibit similar low $^{87}Sr/^{86}Sr$ and moderate ε_{Nd}. They are similar, however, to analysed rocks from Rimatara[28] and Rurutu[29], neighbouring volcanoes in the Austral Islands.

There has been much recent interest in the geographical distribution of isotopic compositions at oceanic islands, culminating in the Dupal anomaly proposal[13], which postulates a region of higher $^{87}Sr/^{86}Sr$, $^{207}Pb/^{204}Pb$ and $^{208}Pb/^{204}Pb$, circling the globe at ~30° S. The new isotopic data for Ua Pou presented

here do not, however, support this view. The Marquesas Islands lie within the proposed Dupal anomaly belt, but only the alkali basalts have the appropriate radiogenic compositions. Apparently both Dupal and non-Dupal mantle reservoirs have been tapped at Ua Pou. The same sequence might also be seen at other French Polynesian islands, if the suspected early tholeiite phase of volcanism could be sampled. Hence, the regional significance of the Dupal anomaly, at least in this area, is questionable (see also refs 8, 26, 30).

It is evident from trace element and isotopic compositions that the tholeiites and alkali basalts at Ua Pou cannot be related by variable degrees of partial melting or crystal fractionation of primary melts from a common mantle or lithospheric source. Thus at least two, and probably three distinct source end-member compositions have contributed to volcanism at this island. In addition, the alkali basalts postdate the tholeiites in a clear age progression implying that the chemically distinct sources were tapped at different times. This suggests that the sources are not ubiquitous and continuously available for melting, but are likely to be physically separate. We will consider two possibilities for the spatial distribution of these source components: first, partial melting of both the mantle plume and the overlying lithosphere, and second, melting of the plume alone. In the first case the lithospheric mantle and plume have differing isotopic compositions and are the sources for the tholeiitic and alkali basalts respectively; in the second, both the alkalic and tholeiitic melts are derived from the plume, implying an isotopically heterogeneous plume.

The lower oceanic lithosphere probably consists of an unmelted mix of enriched mantle blobs and depleted asthenosphere which could possess considerable isotopic heterogeneity[26,31-33] (Fig. 3*a*). Samples from the East Pacific Rise exhibit a rather small range of $^{87}Sr/^{86}Sr$ and ε_{Nd} compositions (Fig. 2*a*), but are quite variable in $^{206}Pb/^{204}Pb$ composition[25,33] (Fig. 2*b*). Variation in these MORB compositions can be explained by mixing melts from depleted upper mantle with those from a small proportion of enriched mantle of the Rurutu/Tubuai type (low $^{87}Sr/^{86}Sr$, moderate ε_{Nd}, high $^{206}Pb/^{204}Pb$). Interestingly, rocks from Easter and Sala y Gomez Islands have compositions at the high-$^{206}Pb/^{204}Pb$ end of this trend[25] (Fig. 2*b*). Mantle upwelling in this region of the East Pacific Rise may be a major source for the enriched mantle blobs which became incorporated into the lower oceanic lithosphere by thickening of the plate during cooling away from the spreading centre.

At Ua Pou we propose that such heterogeneous oceanic lithosphere of 50–60 Myr age approached and crossed the Marquesas hotspot (Fig. 3*a*). Melts and heat from the mantle plume entered the lower lithosphere, where wall rock reached temperatures sufficient to melt. The plume and lithosphere melts could then mix to produce the magmas seen at the island. The trace element and isotopic compositions of the mixed magmas would vary depending on the degree of melting of each source and the proportions of melt contributed. At Ua Pou the isotopic composition of the early tholeiitic phase lies on a mixing line between MORB and Rurutu/Tubuai compositions, and reflects the proposed composition of the lower oceanic lithosphere beneath the island. Hence, in this model, melting of the lower lithosphere was significant and dominates the composition of tholeiitic magmas.

As the volcano migrated away from the hotspot, temperatures at the base of the lithosphere decreased. Smaller degrees of melting (of alkali basalt character) developed in the margin of the plume (Fig. 3*a*). These melts passed through the same column of oceanic lithosphere which had earlier yielded its low-temperature melting fraction; hence, the wall rock was much more refractory and less assimilation occurred at this stage, so that the alkali basalt compositions essentially reflect the isotopic composition of the plume. Contemporaneous with this phase of Ua Pou volcanism was tholeiitic, shield-building volcanism at Hiva Oa, the next major volcano upstream, and perhaps the

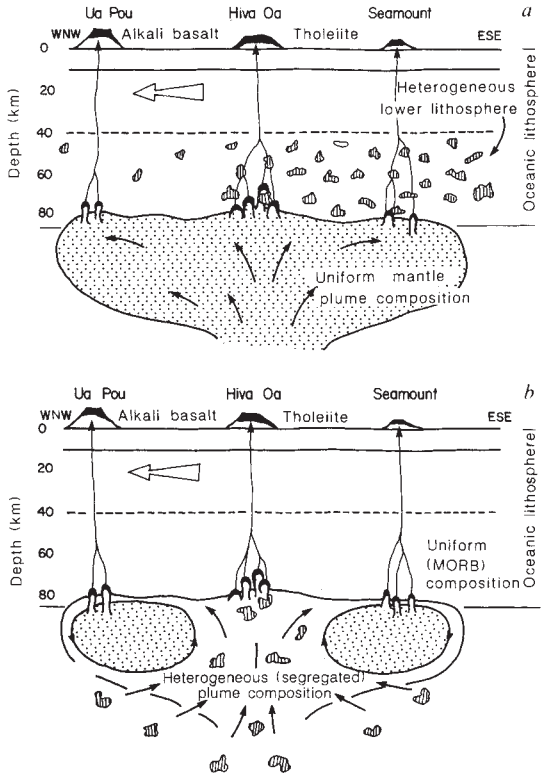

Fig. 3 Two models for the isotopically distinct magmas at Ua Pou, illustrated by vertical cross-sections along the line of the Marquesas Islands. Both models show volcanic activity at ~2.5 Myr, when alkali basalts erupted onto an older tholeiite shield at Ua Pou, concurrently with tholeiitic basalts at Hiva Oa and, possibly, with the initial seamount basalts beneath Fatu Hiva. *a*, Heterogeneous lower lithosphere. The plume (~400 km diameter) has a uniform, undepleted isotopic composition and is crossed by a Pacific plate composed of an upper section of uniform, MORB-like isotopic composition formed at the East Pacific Rise and an isotopically heterogeneous lower lithosphere accreted to the plate as it cooled away from the spreading ridge. Tholeiitic melts are formed over the centre of the plume as melts from the plume mix with melts from the lower-lithosphere wall rock. Alkali basalt melts erupt from the margin of the plume, where temperatures are cooler, and pass through previously heated lithosphere without significant contamination. *b*, Heterogeneous plume. The lithosphere has a uniform, MORB-like isotopic composition throughout and passes over a plume which has developed large-scale chemical heterogeneities by entraining depleted upper mantle material during its diapiric rise[34]. The original plume material concentrates in a torus around the plume margin (shaded), while entrained material flows into the centre[35]. Hence tholeiitic melts from the plume centre are MORB-like in isotopic character, whereas alkali basalt melts from the margin are more like the original plume. The lower lithosphere may melt but the isotopic differences in erupted magmas are controlled by heterogeneities in the plume.

seamount phase at Fatu Hiva, another 100 km to the south-east. From this model we would expect the same correlation of trace element and isotopic composition with time to emerge at other Marquesas islands.

An analogous model for the origin of Hawaiian tholeiitic and alkali basalts has been proposed by Chen and Frey[9]. At Hawaii, however, there is an inverse correlation between $^{87}Sr/^{86}Sr$ and abundances of incompatible elements; that is, the tholeiitic phase is dominated by the composition of melts from the plume, whereas the alkali basalts are thought to reflect the composition of the lower lithosphere. This relationship is thought to result from small degrees of melting of the lower lithosphere and variable proportions of mixing with plume-derived melts[9]. Although lithosphere melting occurs during the tholeiitic phase,

the volume of melts from the plume is sufficiently high that these determine the composition of Hawaiian tholeiites. During the formation of alkali basalt melts, however, very small (<1%) degrees of melting of the wall rock produce high concentrations of trace elements which dominate the composition of small-volume plume melts. Thus the isotopic composition of the Hawaiian alkali basalts reflects that of the lower lithosphere.

The source end-members for melting and magma mixing are different for the two island chains. At Ua Pou the enriched mantle, or plume composition, has $^{87}Sr/^{86}Sr > 0.7053$ and $\varepsilon_{Nd} < 0.5$ and lies to the right of the Sr–Nd mantle array. This may be similar to, but possibly not so extreme as, the plume component for Society Islands alkali basalt magmas[1,12]. The lower lithosphere beneath Hawaii, as reflected by the isotopic composition of the alkali basalts[9], does not appear to contain the Rurutu/Tubuai component seen in the Ua Pou tholeiites. This model therefore requires that the oceanic lithosphere of the Pacific plate has accreted mantle blobs of different isotopic character.

An alternative explanation for the isotopically distinct phases of tholeiitic and alkalic volcanism at Ua Pou is that heterogeneities occur within the plume or diapir itself. These heterogeneities may be either a consequence of initial heterogeneities in the plume source, or result from the incorporation of asthenospheric mantle material into the diapir during its ascent. Recent experimental and theoretical studies[34,35] have demonstrated that thermally activated diapirs will entrain a significant quantity of surrounding mantle material during their ascent. This is illustrated in Fig. 3*b*, where the central portion of the diapir consists of entrained depleted upper mantle (MORB-like plus mantle blobs), while the original plume material is contained in an outer torus. Tholeiitic melts are generated over the centre of the plume while smaller-volume alkali basaltic melts form over the perimeter. If isotopic heterogeneities are distributed uniformly through the diapir, then isotopically distinct magmas could be formed by variable degrees of partial melting. Larger degrees of melting (tholeiite) would tend to homogenize the variable composition of the diapir, whereas smaller degrees of melting (alkali basalt) would emphasize the composition of incompatible-element rich segregations[31,32].

We thank W. F. McDonough for technical assistance and thoughtful discussions, and W. M. White for data in advance of publication. We also thank Y. and J. Hituputoka and J.-L. and C. Candelot for their assistance during fieldwork on Ua Pou. R.A.D. acknowledges the support of NSF and H.G.B. the support of ORSTOM.

Received 17 October 1985; accepted 9 April 1986.

1. White, W. M. & Hofman, A. W. *Nature* **296**, 821–825 (1982).
2. Davies, G. F. *Nature* **290**, 208–213 (1981).
3. Ringwood, A. E. *J. Geol.* **90**, 611–643 (1982).
4. *Basaltic Volcanism on the Terrestrial Planets* (eds Kaula, W. M. *et al.*) 161–192 (Pergamon, New York, 1981).
5. DePaolo, D. J. & Wasserburg, G. J. *Geophys. Res. Lett.* **3**, 743–746 (1976).
6. O'Nions, R. K., Hamilton, P. J. & Evensen, N. M. *Earth planet. Sci. Lett.* **34**, 13–22 (1977).
7. Richard, P., Shimizu, N. & Allègre, C. J. *Earth planet. Sci. Lett.* **31**, 269–278 (1976).
8. White, W. M. *Geology* **13**, 115–118 (1985).
9. Chen, C.-Y. & Frey, F. A. *Nature* **302**, 785–789 (1983).
10. Stille; P., Unruh, D. M. & Tatsumoto, M. *Nature* **304**, 25–29 (1983).
11. Duncan, R. A. & Compston, W. *Geology* **4**, 728–732 (1976).
12. Vidal, Ph., Chauvel, C. & Brousse, R. *Nature* **307**, 536–538 (1984).
13. Hart, S. R. *Nature* **309**, 753–757 (1984).
14. Duncan, R. A. & McDougall, I. *Earth planet. Sci. Lett.* **21**, 414–420 (1974).
15. Brousse, R. & Bellon, H. *C. r. hebd. Séanc. Acad. Sci., Paris* **278**, 827–830 (1974).
16. Epp, D. *J. geophys. Res.* **89**, 11273–11286 (1984).
17. Bishop, A. C. & Woolley, A. R. *Contr. Miner. Petrol.* **39**, 309–326 (1973).
18. Liotard, J. M., Barsczus, H. G., Dupuy, C. & Dostal, J. *Contr. Miner. Petrol.* **92**, 260–268 (1986).
19. Macdonald, G. A. & Katsura, T. *J. Petrol.* **5**, 82–133 (1964).
20. Barsczus, H. G. *Notes Doc. (Géophys.) ORSTROMA Papeete* **1981**, 1–22 (1981).
21. Barsczus, H. G & Liotard, J. M. *C.r. hebd. Séanc. Acad. Sci., Paris* **300**, 915–918 (1985).
22. Frey, F. A. & Clague, D. A. *Earth planet. Sci. Lett.* **66**, 337–355 (1983).
23. Leeman, W. P., Budahn, J. R., Gerlach, D. C., Smith, D. R. & Powell, B. N. *Am. J. Sci.* **280A**, 794–819 (1980).
24. Wright, T. L. *J. geophys. Res.* **89**, 3233–3252 (1984).
25. White, W. M. *EOS* **66**, 408 (1985).
26. McDonough, W. F., McCulloch, M. T. & Sun, S.-S. *Geochim. cosmochim. Acta* **49**, 2051–2068 (1985).
27. Nelson, D. R., McCulloch, M. T. & Sun, S.-S. *Geochim. cosmochim. Acta* **50**, 231–246 (1986).
28. Tatsumoto, M., Unruh, D. M., Stille, P. & Fujimaki, H. *Proc. 27th int. Geol. Congr.* **11**, 485–501 (1984).
29. Palacz, Z. & Saunders, A. D. *Abstr. int. Volcanol. Congr.* Feb., 194 (1986).
30. McDonough, W. F. *et al. Abstr. int. Volcanol. Congr.* Feb., 180 (1986).
31. Zindler, A., Staudigel, H. & Batiza, R. *Earth planet. Sci. Lett.* **70**, 175–195 (1984).
32. Staudigel, H. *et al. Earth planet. Sci. Lett.* **69**, 13–29 (1984).
33. Hamelin, B., Dupré, B. & Allègre, C. J. *Earth planet. Sci. Lett.* **67**, 340–350 (1984).
34. Griffiths, R. W. *Earth planet. Sci. Lett.* (submitted).
35. Griffiths, R. W. *Phys. Earth planet. Inter.* (submitted).

Geophysical evidence for the East Antarctic plate boundary in the Weddell Sea

Yngve Kristoffersen & Kristen Haugland

Seismological Observatory, University of Bergen, Allègt. 41, 5000 Bergen, Norway

An improved Gondwanaland reconstruction compatible with geological and geophysical information from the surrounding oceans and continents seems to require microplates to solve the enigmatic pre-early-Mesozoic tectonic relation between West and East Antarctica[1]. New multi-channel seismic reflection data from the southeastern Weddell Sea acquired during the 1984–85 Norwegian Antarctic Research Expedition (NARE) have outlined a linear WSW–ENE-trending basement ridge buried below the continental slope over a distance of 700 km. This structural high truncates the trend of the large sedimentary basins below the Filchner and Ronne ice shelves and may continue to within a few hundred kilometres of the Antarctic Penninsula. We interpret the basement ridge as part of the East Antarctic plate boundary during the break-up of Gondwana. The morphology and structure of this boundary show greater apparent similarity to a rifted or obliquely rifted margin than to the sheared margin which is predicted by current reconstructions[2,3]. A linear East Antarctic plate margin extending to the vicinity of the Antarctic Peninsula makes any post-rift microplate motion in the Weddell Embayment unlikely.

Major linear basement highs have been found below the lower continental slope of the southeastern Weddell Sea margin (Fig. 1). In the north-east, the Explora Escarpment[4] is characterized by a well-defined 10–20-km-wide basement ridge of 1–2 km elevation with respect to hyperbolated acoustic basement on the seaward side (Fig. 2). On the landward side, a wedge of seaward-dipping seismic reflectors, the Explora wedge, unconformably overlain by a 1–2-km-thick section of nearly flat-lying seismic sequences, abuts the ascarpment. Towards the south-west (20 °W), the Explora Escarpment becomes more subdued. The new NARE seismic data demonstrate that a major basement structure collinear with the Explora Escarpment extends at least 700 km farther towards the south-west, but also reveal considerable lateral variation in basement morphology (Figs 1, 2). Between 19 and 23° W a sharp, piece-wise-continuous reflector forms the upper boundary of a sequence of low-frequency seismic reflections whose landward termination is abrupt in some places and more diffuse in others (Fig. 3). We interpret these seismic reflection events as representing a region of seaward-dipping lava flows. We note that the top of this sequence is at a level comparable to the top of the escarpments to the north-east and west.

Further west, between 23 and 25° W, is a zone where acoustic basement forms a steep, landward-facing escarpment with down-faulted blocks of lava flows (?) at its base (Fig. 2, line 22–85). Here the escarpment appears to be offset from the landward boundary of the lava pile to the north-east.

At 26° W, the WSW-trending collinear basement structure is a subdued, 15–30-km-wide ridge with a relief of ~600 m which increases westwards to >2,000 m at 32° W (Fig. 2). We name the basement structure between 23 and 38° W the Andenes